ISSN 0023-1584, Kinetics and Catalysis, 2012, Vol. 53, No. 4, pp. 449–455. © Pleiades Publishing, Ltd., 2012.
Original Russian Text © S.N. Vereshchagin, E.V. Kondratenko, E.V. Rabchevskii, N.N. Anshits, L.A. Solov'ev, A.G. Anshits, 2012, published in Kinetika i Kataliz, 2012, Vol. 53, No. 4, pp. 470–476.

New Approach to the Preparation of Catalysts for the Oxidative Coupling of Methane

S. N. Vereshchagin[a], E. V. Kondratenko[b], E. V. Rabchevskii[a], N. N. Anshits[a], L. A. Solov'ev[a], and A. G. Anshits[a]

[a] *Institute of Chemistry and Chemical Technology, Siberian Branch, Russian Academy of Sciences, Krasnoyarsk, 660036 Russia*
[b] *Leibniz Institute for Catalysis at the University of Rostock (LIKAT), Rostock, Germany*
e-mail: snv@icct.ru

Received November 30, 2011

Abstract—A new approach to the preparation of systems that exhibit catalytic activity in the oxidative coupling of methane (OCM) is considered. With the use of ferrospheres separated from power-generation ashes from different sources as an example, it was demonstrated that OCM catalysts can be prepared by the crystallization/solidification of oxide melts with the formation of microspherical particles. The dependence of activity and selectivity for the oxidative reforming of methane on the ferrospheres containing from 36.2 to 92.5 wt % Fe_2O_3 into the products of deep oxidation and OCM was studied. It was found that deep oxidation reactions on ferrospheres with Fe_2O_3 contents higher than 85% were suppressed, and the main reaction path of CH_4 conversion was its oxidative coupling with the formation of C_2 products (with selectivity to 60% at 750°C); moreover, the selectivity for C_2 formation in this region was proportional to the concentration of Fe_2O_3. Phases responsible for the catalytic conversion of methane into CO_x and OCM products were considered, and it was shown that the catalytic activity and selectivity of the oxidative transformation of CH_4 on ferrospheres is determined by the position of the point that corresponds to their composition on a phase diagram of $CaO–Fe_2O_3–SiO_2$.

DOI: 10.1134/S0023158412040131

INTRODUCTION

The oxidative coupling of methane (OCM) is an attractive method for the conversion of the most inert hydrocarbon in natural gas—methane—into valuable chemical products, primarily, ethylene. The minimum economically sound OCM process efficiency should provide a C_2H_4 yield of 16–30% at >80% selectivity for methane conversion, depending on the cost of ethylene [1, 2]. In spite of the fundamental limitation according to which the yield of C_2^+ products in OCM cannot be higher than 28–30%, search for new catalysts, an improvement to the currently available catalysts, and a refinement of the process (use of membrane reactors, distributed introduction of the oxidizing agent, etc.) are being continued on a global scale [3, 4]. Because the cost of the catalyst is a measure of the economic efficiency of the OCM process as a whole, search for inexpensive systems that can provide the necessary level of methane conversion into C_2 products undoubtedly remains a problem of considerable current interest.

Currently, the majority of supports and catalysts are mainly prepared by methods that include wet stages of precipitation, impregnation, etc. Any multistage technological cycle involves the resource- and energy-consuming stages of filtration, washing, drying, molding, and calcination, and solutions that should be neutralized and utilized form in the course of the process. As a rule, the aim of a sequence of technological operations is to prepare catalysts with high specific surface areas, a small particle size of the active constituent, and significant porosity, that is, to impart properties that do not play the determining role in the reaction of methane conversion into C_2 products to the catalysts. It is well known that the catalyst should possess a low specific surface area and an optimum pore structure dominated by wide pores of size 10^{-2}–10^{-3} cm for the optimum run of the heterogeneous–homogeneous OCM reaction [4]. It is particularly desirable to have spherical particles with high thermal stability and mechanical strength, which make it possible to perform a process in both a fixed bed with the minimum flow resistance and a fluidized bed with more efficient heat transfer.

The treatment of an oxide mixture in a high-temperature turbulent flow, when melting, dispersion, and the consolidation of melt drops with the formation of spheroid particles occur in the course of a single technological stage, is a method for preparation of spherical particles. An obvious difficulty in applying this approach to the synthesis of catalysts is the need for forcing the crystallizing melt to form a catalytically active phase.

The described melting–dispersion–consolidation process accompanies the high-temperature combus-

tion of powdered coal at power plants with the passage of the stage of the complete melting of the mineral components of coal. As a result, so-called fly ash is formed as a by-product, which consists of a mixture of microspherical particles; this mixture can be separated into individual size fractions of similar mineral-phase and chemical compositions [5]. Earlier, it was found that some fractions of microspheres separated from fly ash exhibit noticeable catalytic activity both in the process of deep oxidation and in the OCM reaction [6–8]. So-called ferrospheres (microspheres with high iron oxide contents to 93 wt %) are most active in the OCM reaction; moreover, modified ferrospheres approach the best synthetic systems in terms of activity and selectivity (the degree of methane conversion, to 24%; the selectivity for the formation of C_2 products, to 70%) [9], but they are much less expensive. It is obvious that the regularities of the formation of particles that possess catalytic activity in the OCM reaction can serve as a basis for evaluating prospects for the practical use of a process of the preparation of microspherical OCM catalysts by the crystallization of dispersed oxide melts.

The aim of this work was to study the catalytic activity of ferrospheres and the formation of phases that exhibit activity in the oxidative reforming of methane in them using a number of iron-containing microspheres with different chemical and phase compositions as an example.

EXPERIMENTAL

The narrow size fractions of ferrospheres were separated from magnetic concentrates, which, in turn, were obtained from fly ash formed upon the combustion of pulverized coals from the Kuznetsk (P2), Ekibastuz (E), Tugnuiskoe (B1), and Berezovo (S1) deposits. Dry and wet magnetic separation in fields of different intensities, hydrodynamic separation, and granulometric classification were used for the isolation of ferrospheres. The separation process was described in detail elsewhere [10]. The separated fractions were the mixtures of spherical particles with a specified size, and the concentrations of globules whose size was smaller or greater than the specified value did not exceed 10%. According to this procedure, more than 100 different products were obtained, from which 19 uniform narrow fractions of ferrospheres with different total Fe_2O_3 contents and particle sizes were chosen for the catalytic experiments (table). In terms of the range of compositions, this series of samples was superior to all of the previously studied series of fractions of ferrospheres, magnetic concentrates [11–18], and individual globules [15].

The purity of fractions was controlled with an Axio Imager D1 optical microscope equipped with an AxoiCam MRc5 digital color video camera.

The chemical composition of the narrow fractions of microspherical products (see the table) was analyzed according to GOST (State Standard) 5382-91; the errors of determinations were the following %, SiO_2 ±0.35, Al_2O_3 ±0.2, Fe_2O_3 ±0.6; CaO, ±0.15; MgO, ±0.2; Na_2O ±0.1, K_2O ±0.15, and TiO_2 ±0.07. Henceforth, the iron content of the samples is specified in terms of Fe_2O_3 regardless of the real chemical species present in ferrospheres (Fe_3O_4, etc.).

The catalytic properties of the narrow fractions of ferrospheres were studied in a HECTOR catalytic flow multireactor system. The initial mixture and the products of methane conversion were analyzed on an Agilent 6890 multicolumn chromatograph, which makes it possible to quantitatively determine light gases (H_2, CO, O_2, N_2, and CO_2), water, and individual C_1–C_5 hydrocarbons.

The experiments were carried out at temperatures from 600 to 750°C, the volumetric composition of the reaction mixture of $CH_4 : O_2 : N_2 = 82 : 9 : 9$, and a total pressure of 1.3 atm. The weight of ferrospheres was 0.30–0.33 g, and the flow rate of the mixture converted to normal conditions was 15 cm^3/min. To study the temperature dependence of the activity of catalysts, they were consecutively heated in a flow of the reaction mixture to 600, 650, 700, and 750°C and were kept at each temperature for about 4 h (for 15 h at 700°C).

The quantitative phase composition of ferrospheres was determined by X-ray powder diffraction using the full-profile Rietveld method [19] and refinement by derivative difference minimization [20]. The X-ray diffraction patterns were measured in reflection geometry with the use of CoK_α radiation on a PANalytical X'Pert PRO diffractometer with a PIXcel detector and a graphite monochromator. X-ray diffraction patterns were obtained in the 2θ range from 15 to 115°C. The weight concentration of an X-ray amorphous phase (%) was determined by an external standard method with the use of hematite. The absorption coefficients of the samples with respect to CoK_α radiation were calculated based on the overall elemental composition found by chemical analysis. For controlling the reproducibility of the results, NaCl as an internal standard was added to some samples.

The specific surface areas of the samples were determined from the thermal desorption of nitrogen on a NOVA 3200e automatic analyzer using the multipoint BET method.

RESULTS AND DISCUSSION

Chemical Composition and Catalytic Properties of the Ferrospheres

Figure 1 shows the photographs of three fractions of ferrospheres of different sizes. The particles of all of the samples were spheroidal; small inclusions of nonspherical and defective particles were also present. As follows from the above table, the main components of the test ferrospheres were the oxides of iron (36.2–

Chemical composition of ferrospheres chosen for studying their catalytic properties

Sample no.	Sample*	S_{sp}, m^2/g	Loss on ignition, %	Chemical composition, wt %								
				SiO_2	Al_2O_3	Fe_2O_3	CaO	MgO	Na_2O	K_2O	TiO_2	SO_3
1	S1(0.4–0.2)	0.21	0.00	4.00	1.90	85.20	8.69	1.00	0.25	0.07	0.18	0.25
2	S1(0.2–0.16)	0.21	0.00	2.48	1.20	88.42	7.43	0.81	0.20	0.05	0.19	0.21
3	S1(0.16–0.1)	0.17	0.00	1.26	0.83	92.52	4.90	1.30	0.11	0.04	0.17	0.27
4	S1(0.1–0.063)	0.19	0.00	1.30	0.92	90.47	6.60	0.90	0.20	0.06	0.18	0.28
5	S1(0.063–0.05)	0.18	0.00	1.35	1.02	89.25	6.70	0.81	0.24	0.10	0.12	0.28
6	S1(<0.05)	0.35	0.00	0.64	0.92	89.12	8.81	0.60	0.10	0.05	0.16	0.25
7	B1(0.1–0.063)	0.38	0.00	9.00	6.22	79.12	5.40	0.90	0.23	0.08	0.10	0.26
8	B1(0.063–0.05)	0.44	0.00	9.50	4.64	76.24	9.08	0.81	0.20	0.07	0.19	0.29
9	B1(<0.05)	0.50	0.00	9.41	5.04	78.38	6.24	1.10	0.20	0.05	0.16	0.24
10	E(0.4–0.2)	3.53	2.56	39.70	15.92	36.26	3.69	1.38	0.40	0.26	1.14	0.60
11	E(0.2–0.16)	1.76	1.70	36.91	15.16	41.26	3.25	1.64	0.80	0.26	1.15	0.71
12	E(0.16–0.1)	2.40	1.26	38.40	16.32	39.31	2.82	1.61	0.25	0.20	1.03	0.46
13	E(0.1–0.063)	1.55	0.32	33.08	12.74	49.28	2.71	1.15	1.18	0.26	1.28	0.62
14	E(0.063–0.05)	1.03	0.00	26.48	9.44	59.82	2.82	1.08	0.94	0.20	1.40	0.67
15	E(<0.05)	0.86	0.00	19.20	8.39	71.32	1.96	1.01	0.10	0.13	0.00	0.02
16	P2(0.16–0.1)	3.23	2.11	37.67	12.96	37.47	5.81	2.92	0.66	0.66	0.23	0.22
17	P2(0.1–0.063)	2.44	1.58	33.90	8.82	48.93	2.94	3.38	0.75	0.45	0.00	0.05
18	P2(0.063–0.05)	1.65	0.00	23.84	8.52	61.42	3.17	2.87	0.80	0.40	0.00	0.05
19	P2(<0.05)	2.02	0.12	20.70	6.62	66.38	2.94	2.82	0.80	0.40	0.05	0.04

* S1, B1, E, and P2 refer to the origin of fly ashes (coals from the Berezovo, Tugnuiskoe, Ekibastuz, and Kuznetsk deposits, respectively); the sizes of ferrosphere fractions in mm are given in parentheses (the former and latter numerals correspond to the greatest and smallest mesh sizes of the sieves used for fractionation).

92.5 wt %), silicon (0.64–39.7 wt %) and aluminum (0.83–16.3 wt %), the total concentration of which was 87.7–98.9 wt %, and also to 9.1% calcium oxide. The concentrations of SiO_2, Al_2O_3, and Fe_2O_3 varied over wide ranges, but these changes are not independent; the following linear correlation is observed in the series of ferrospheres given in the table:

$$C_{SiO_2} = (2.71 \pm 0.32)C_{Al_2O_3}, \quad (1)$$

where C_{SiO_2} and $C_{Al_2O_3}$ are the concentrations (%) of SiO_2 and Al_2O_3 oxides, respectively.

Because the total concentration of Al_2O_3, SiO_2, and Fe_2O_3 is about 90% or higher in all cases, it is obvious that the macrocomponent composition of ferrospheres can be expressed by the only concentration parameter. It is most reasonable to choose the concentration of Fe_2O_3 as this parameter because Fe_2O_3 is the component of many catalysts for redox processes.

The noticeable transformation of methane and oxygen on all of the test samples began at temperatures higher than 600°C. The catalytic activity of the samples in the oxidative conversion of CH_4 changed in a wide range. It was quantitatively characterized by the degree of conversion of oxygen (x_{ox}) as a component that occurred in deficiency in the reaction mixture. The dependence of the conversion of methane (x_m) on the concentration of Fe_2O_3 qualitatively coincided with the corresponding curves for oxygen, but changes were more weakly pronounced: upon varying x_{ox} from 0 to 100%, changes in x_m did not exceed 8%.

Figure 2 shows the dependence of the catalytic activity of ferrospheres at 700°C on the total Fe_2O_3 content of the samples ($C_{Fe_2O_3}$). In spite of the considerable scatter of experimental data caused by the different origins of the samples, it is obvious that the activity regularly changed with $C_{Fe_2O_3}$, although these

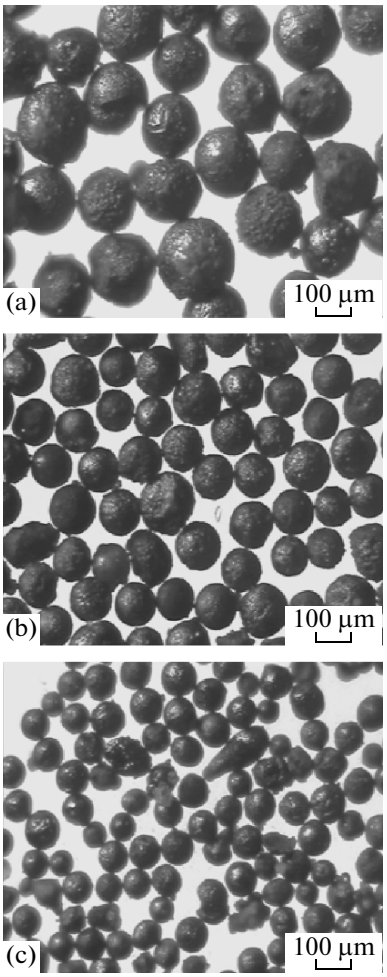

Fig. 1. Optical micrographs of ferrosphere fractions: (a) S1(0.2–0.16), (b) S1(0.16–0.1), and (c) S1(0.063–0.05).L

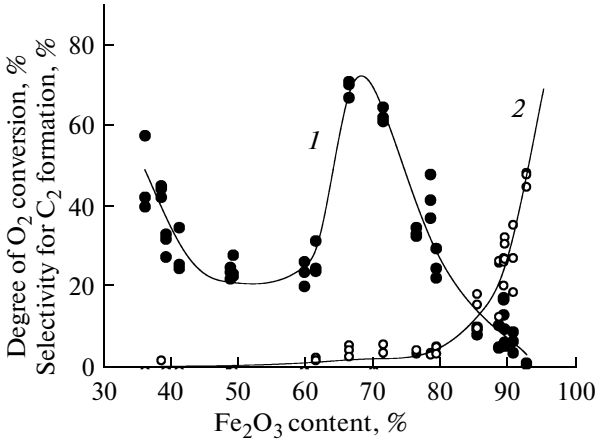

Fig. 2. Dependence of (*1*) the catalytic activity and (*2*) selectivity for the formation of C_2 products at 700°C on the total iron content of the ferrospheres.

changes were complicated and nonmonotonic. At $C_{Fe_2O_3}$ = 65–70%, a maximum was observed, which also manifested itself at temperatures of 600 and 750°C.

The selectivity of methane conversion also substantially depended on the concentration of Fe_2O_3 (Fig. 2). The main products of CH_4 conversion on the samples with $C_{Fe_2O_3} < 80\%$ were CO and CO_2, whereas these were ethane, ethylene, and C_3 hydrocarbons at Fe_2O_3 concentrations higher than 80%. In this region of the composition of ferrospheres, the selectivity of the formation of OCM products increased with temperature, whereas the selectivity of the formation of C_2 hydrocarbons at a constant temperature was proportional to $C_{Fe_2O_3}$, and it reached 60% on the samples with high iron oxide content at 750°C.

Note that, in the series of the studied ferrospheres, an almost monotonic decrease in the specific surface area from 3.5 to 0.17 m^2/g was observed as $C_{Fe_2O_3}$ was increased (see the table). Therefore, an extremum in the curve of catalytic activity (Fig. 2) and a sharp increase in selectivity in the OCM reaction should be primarily related to changes in the chemical and phase compositions of the surfaces of ferrospheres depending on their gross composition.

Based on data given in Fig. 2, all of the ferrospheres can be tentatively subdivided into the following three groups according to their behaviors in the oxidative conversion of methane:

Group I. It includes the samples in which $C_{Fe_2O_3} <$ 65%. The activity of these ferrospheres is low, and the deep oxidation of methane makes the greatest contribution.

Group II. The samples from this group (with $C_{Fe_2O_3}$ = 65–80%) are active but nonselective catalysts for OCM. The processes of deep methane oxidation to CO_2 mainly occur on them, and ferrospheres with the Fe_2O_3 content of about 70% exhibit a maximum activity.

Group III. This group contains samples with the Fe_2O_3 content higher than 80%; increased selectivity for the formation of C_2 products (30–60%), which increases with the total Fe_2O_3 content, is observed on them.

Phase Composition of the Ferrospheres

The X-ray diffraction study of ferrospheres showed that phases with the spinel structure (spinel-type ferrite and magnetite) and hematite were the main crystalline phase constituents of the initial samples. They accounted for 40 to 90% of the sample weights, whereas the fractions of quartz and mullite were to 10 and to 4%, respectively. The concentration of amorphous or weakly crystalline phases varied from 8 to 57%. Under reaction conditions at 600–750°C, the oxidation of a portion of magnetite to hematite, which is thermodynamically more stable in the presence of oxygen at lower temperatures, was observed in all of the samples.

It is interesting that the unit cell parameters of hematite (a, c) and the spinel-type ferrite phase (a_0) increased with the total Fe_2O_3 content. In this case, the slopes of the regression lines of parameters a_0 (Fig. 3), a, and c as functions of iron content exhibited a pronounced break at $C_{Fe_2O_3}$ = 65–70%, which approximately corresponds to the boundary of a transition from group I samples to group II ferrospheres. At high Fe_2O_3 contents, the parameters a_0, a, and c approached the corresponding values for individual α-Fe_2O_3 and Fe_3O_4 or became greater than they in the case of group III samples (Fig. 3).

It is most likely that hematite and/or magnetite (spinel-type ferrite), which are inactive in the OCM reaction [9] and known as catalysts for the complete oxidation of hydrocarbons [21], are phases responsible for the catalytic activity of ferrospheres in the reaction of deep oxidation. The currently available experimental data cannot unambiguously explain the origin of a maximum in the region of 60–80% in the dependence of catalyst activity on the iron oxide content; however, is possible to assume that this is caused by the joint action of several factors:

—an increase in the total amount of an active spinel-type ferrite phase with the concentration of iron oxides in the system;

—a change in the composition of spinel-type ferrite, primarily, a decrease in the concentration of aluminum in solid solutions based iron oxides; it is well known that extensive regions in the phase diagram of $FeO–Fe_2O_3–Al_2O_3$ correspond to these solid solutions [22];

—different degrees of blocking of the surface of an active phase by an amorphous (low-crystalline) component of the system; in particular, a vitreous phase can serve as this component.

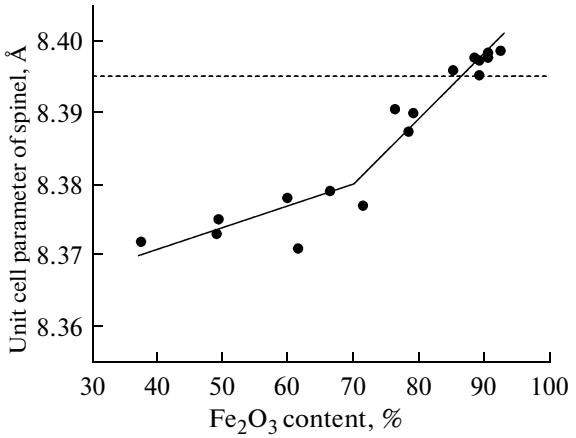

Fig. 3. Dependence of the lattice parameter of spinel after performing catalytic experiments on the samples upon the total Fe_2O_3 content. The dashed line corresponds to the parameter a_0 of individual Fe_3O_4.

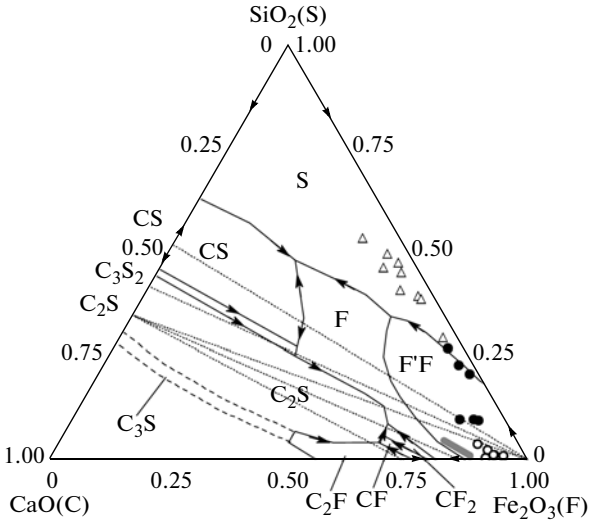

Fig. 4. Projection of ferrosphere compositions on the phase diagram of the $CaO–Fe_2O_3–SiO_2$ system. Ferrospheres from the first, second, and third groups are marked with Δ, ●, and ○ respectively. CS is $CaSiO_3$, F'F – Fe_3O_4, C_2F is $Ca_2Fe_2O_5$, CF is $CaFe_2O_4$, and CF_2 is $CaFe_4O_7$. The region corresponding to the stability zone of the silicoferrites of calcium is shaded.

Effect of the Formation Conditions of the Ferrospheres on Their Catalytic Activity

Because the total concentration of SiO_2, CaO, Fe_2O_3, and Al_2O_3 oxides in all of the samples was no lower than 93% (see the table), the formation of the phase composition of ferrospheres upon the solidification of the drops of a melt should be correlated with the phase diagram of the $CaO–FeO–Fe_2O_3–Al_2O_3–SiO_2$ system. However, the region of $Fe_2O_3–FeO$ is poorly known; moreover, Al_2O_3 is usually not considered as a mineral-forming oxide in the test system [23]. Taking into account these facts, as a first approximation, we can lower the rank of the system by considering processes that occur in ferrospheres in the $CaO–Fe_2O_3–SiO_2$ coordinates. Figure 4 schematically shows the phase diagram of this system [24]. Points that correspond to the projections of test sample compositions on the $CaO–Fe_2O_3–SiO_2$ plane are shown in this diagram. It can be seen that three groups of ferrospheres with different catalytic properties are located in the parts of the diagram that correspond to the crystallization of different primary products.

The group I ferrospheres fall into the region of the compositions that correspond to the primary crystallization of SiO_2 (Fig. 4, mark Δ). With consideration for the nonequilibrium character of crystallization and the high viscosity of an aluminosilicate melt in this

region, is possible to assume that the mixture is solidified with the predominant formation an amorphous (vitreous) phase; this is confirmed by the high concentrations of a vitreous phase in the samples of group I ferrospheres. The resulting vitreous phase blocks the crystallites of active iron-containing phases (spinel-type ferrite and hematite); this decreases the catalytic activity of the samples of this group in the oxidative conversion of CH_4.

At $C_{Fe_2O_3} \approx 70\%$, the sample composition curve intersects a cotectic boundary line and falls into the field of primary crystallization of Fe_2O_3–Fe_3O_4. This concentration of iron oxides corresponds to an inflection point in the curve of a_0 as a function of $C_{Fe_2O_3}$ (Fig. 3), which is indicative of qualitative changes in the formation conditions of iron-containing phases.

The samples from the second group are entirely located in the region of compositions corresponding to the primary crystallization of Fe_2O_3–Fe_3O_4 (Fig. 4, mark ●). Although the end point of the crystallization process (the CS–S–F ternary eutectic system) coincides with the corresponding point for the ferrospheres of the first group, the formation of phases occurs at another ratio between components in the region with a pronounced tendency toward the formation of vitreous-crystalline compositions. Correspondingly, a maximum amount of spinel-type ferrite, that is, a phase active in the reaction of deep oxidation, which is screened by a vitreous phase to a minimum degree, is formed in the samples of this group. Calcium, which occurs in the melt, is primarily included in the composition of silicates.

The iron-rich melts, whose composition corresponds to the composition of ferrosphere samples from the third group, are also located in the region of the primary crystallization of magnetite–hematite near the Fe_2O_3 corner of the phase diagram of the CaO–Fe_2O_3–SiO_2 system (Fig. 4, mark ○). The equilibrium crystallization of these compositions is complete at the triple eutectic point of Fe_2O_3–$CaFe_4O_7$–Ca_2SiO_4 at 1216°C. Calcium in these samples is not only precipitated as silicates but also included in iron–calcium compositions. These compositions are either metastable (like solid solutions based on spinel-type ferrite and hematite) with an increase in the crystal lattice parameters of spinel-type ferrite and hematite in the group III samples, as compared with the values of a_0, a, and c in individual Fe_3O_4 and α-Fe_2O_3, or relatively stable, like the silicoferrites of calcium [25], whose subsolidus zone of stability is shown in Fig. 4. It is believed that these iron–calcium components are responsible for the selectivity of the oxidative conversion of methane and the occurrence of the OCM reaction.

CONCLUSIONS

Thus, based on the results of this study, we can make the following conclusions:

(1) Microspherical catalysts for the high-temperature oxidative conversion of methane can be prepared in a single step in the process of melting–dispersion–solidification of an oxide mixture.

(2) The catalytic activity of ferrospheres in OCM is caused by iron–calcium components, which are formed at the stage of the solidification of a molten oxide mixture.

(3) At the total Fe_2O_3 content of ferrospheres higher than 80 wt %, the selectivity for the formation of C_2 products is proportional to the total Fe_2O_3 content to reach 60%.

REFERENCES

1. Kondratenko, E.V., *"Future Feedstocks for Fuels and Chemicals," DGMK Conf.,* Berlin, 2008, p. 45.
2. Gradassi, M.J. and Green, W.N., *Fuel Process. Technol.*, 1995, vol. 42, nos. 2–3, p. 65.
3. Kondratenko, E.V. and Baerns, M., in *Handbook of Heterogeneous Catalysis*, Ertl, G., Knözinger, H., Schüth, F., and Weitkamp, J., Eds., Weinheim: Wiley-VCH, 2008, vol. 8, p. 3010.
4. Arutyunov, V.S. and Krylov, O.V., *Okislitel'nye prevrashcheniya metana* (Oxidation Reactions of Methane), Moscow: Nauka, 1998.
5. Sharonova, O.M., Vereshchagina, T.A., Anshits, N.N., Anshits, A.G., Rabchevskii, E.V., Zykova, I.D., Akimochkina, G.V., Burdin, M.V., and Kryuchik, D.M., *Tekh. Mashinostr.,* 2003, vol. 1, no. 41, p. 66.
6. Vereshchagin, S.N., Anshits, N.N., Salanov, A.N., Sharonova, O.M., Vereshchagina, T.A., and Anshits, A.G., *Chem. Sustainable Dev.*, 2003, vol. 1, p. 303.
7. Wang, S., *Environ. Sci. Technol.*, 2008, vol. 42, no. 19, p. 7055.
8. Fomenko, E.V., Kondratenko, E.V., Salanov, A.N., Bajukov, O.A., Talyshev, A.A., Maksimov, N.G., Nizov, V.A., and Anshits, A.G., *Catal. Today*, 1998, vol. 42, no. 3, p. 267.
9. Fomenko, E.V., Kondratenko, E.V., Sharonova, O.M., Plekhanov, V.P., Koshcheev, S.V., Boronin, A.I., Salanov, A.N., Bajukov, O.A., and Anshits, A.G., *Catal. Today*, 1998, vol. 42, no. 3, p. 273.
10. RF Patent 2407595.
11. Kizil'shtein, L.Ya., Dubov, I.V., Shpitsgluz, A.L., and Parada, S.G., *Komponenty zol i shlakov TES* (Components of Ash and Slag from Heat Power Plants), Moscow: Energoatomizdat, 1995.
12. Vassilev, S.V., *Fuel*, 1992, vol. 71, no. 6, p. 625.
13. Vassilev, S.V., Menendez, R., Borrego, A.G., Diaz-Somoano, M., and Rosa Martinez-Tarazona, M., *Fuel*, 2004, vol. 83, nos. 11–12, p. 1563.
14. Hower, J.C., Rathbone, R.F., Robertson, J.D., Peterson, G., and Trimble, A.S., *Fuel*, 1999, vol. 78, no. 2, p. 197.

15. Sokol, E.V., Kalugin, V.M., Nigmatulina, E.N., Volkova, N.I., Frenkel, A.E., and Maksimova, N.V., *Fuel*, 2002, vol. 81, no. 7, p. 867.
16. Kukier, U., Ishak, C.F., Sumner, M.E., and Miller, W.P., *Environ. Pollut.*, 2003, vol. 123, no. 2, p. 255.
17. Bibby, D.M., *Fuel*, 1977, vol. 56, no. 4, pp. 427–431.
18. Dai, S., Zhao, L., Peng, S., Chou, C.L., Wang, X., Zhang, Y., Li, D., and Sun, Y., *Int. J. Coal Geol.*, 2010, vol. 81, no. 4, p. 320.
19. Rietveld, H., *J. Appl. Crystallogr.*, 1969, vol. 2, no. 2, p. 65.
20. Solovyov, L., *J. Appl. Crystallogr.*, 2004, vol. 37, no. 5, p. 743.
21. Boreskov, G.K., *Kataliz: Voprosy teorii i praktiki: Izbrannye trudy* (Catalysis Theory and Practice: Selected Works), Novosibirsk: Nauka, 1987.
22. Berezhnoi, A.S., *Mnogokomponentnye sistemy okislov* (Multicomponent Oxide Syatems), Kiev: Naukova Dumka, 1970.
23. Malysheva, T. and Mansurova, N., *Russ. Metall.*, 2008, vol. 2008, no. 2, p. 93.
24. Levin, E.M., Robbins, C.R., and McMurdie, H.F., *Phase Diagrams for Ceramists*, Columbus, Ohio: Am. Ceram. Soc., 1964.
25. Patrick, T.R.C. and Pownceby, M.I., *Metall. Mater. Trans. B*, 2002, vol. 33, no. 1, p. 79.